Evidence for electron-phonon interaction in $Fe_{1-x}M_xSb_2$ (M=Co and Cr; $0 \leq x \leq 0.5$) single crystals

N. Lazarević and Z. V. Popović
Center for Solid State Physics and New Materials, Institute of Physics, Pregrevica 118, 11080 Belgrade, Serbia

Rongwei Hu* and C. Petrovic
Condensed Matter Physics and Materials Science Department, Brookhaven National Laboratory, Upton, New York 11973-5000, USA

(Received 3 December 2009; revised manuscript received 2 March 2010; published 16 April 2010)

We have measured polarized Raman scattering spectra of the $Fe_{1-x}Co_xSb_2$ and $Fe_{1-x}Cr_xSb_2$ ($0 \leq x \leq 0.5$) single crystals in the temperature range between 15 and 300 K. The highest energy B_{1g} symmetry mode shows significant line asymmetry due to phonon-mode coupling-width electronic background. The coupling constant achieves the highest value at about 40 K and after that it remains temperature independent. Origin of additional mode broadening is pure anharmonic. Below 40 K the coupling is drastically reduced, in agreement with transport properties measurements. Alloying of $FeSb_2$ with Co and Cr produces the B_{1g} mode narrowing, i.e., weakening of the electron-phonon interaction. In the case of A_g symmetry modes we have found a significant mode mixing.

DOI: 10.1103/PhysRevB.81.144302 PACS number(s): 78.30.Hv, 72.20.−i, 75.20.−g, 73.63.−b

I. INTRODUCTION

$FeSb_2$ is a narrow-gap semiconductor which attracted a lot of attention because of its unusual magnetic,[1] thermoelectric,[2] and transport properties.[3] The magnetic susceptibility of $FeSb_2$ is nearly constant at low temperatures with paramagnetic-to-diamagnetic crossover at around 100 K for a field applied along the c axis, similar to FeSi.[3] The electrical resistivity along the a and b axes shows semiconducting behavior with rapid increase for $T<100$ K. Along the c axis resistivity exhibits a metal to semiconductor transition at around 40 K.[1,4] Based on the measurements of the electrical resistivity, magnetic susceptibility, thermal expansion, heat capacity, and optical conductivity the $FeSb_2$ has been characterized as a strongly correlated semiconductor.[1–6] It was also shown that $FeSb_2$ has colossal Seebeck coefficient S at 10 K and the largest power factor $S^2\sigma$ ever reported.[2] Thermal conductivity κ of $FeSb_2$ is relatively high and is dominated by phonons around 10 K with phonon mean-free path $l_{ph} \sim 10^2$ μm several orders of magnitude larger than electronic mean-free path.[2]

In the recent room-temperature study we have observed all six Raman active modes of $FeSb_2$ predicted by theory.[7] Racu *et al.*[8] measured polarized Raman scattering spectra of $FeSb_2$ single crystals below room temperature and found only anharmonicity of A_g and B_{1g} symmetry modes with no additional electron-phonon coupling.

In this work we have measured at different temperatures polarized Raman scattering spectra of pure $FeSb_2$ single crystals and $FeSb_2$ crystals alloyed with Co and Cr. The B_{1g} mode asymmetry and broadening is analyzed using Breit-Wigner-Fano (BWF) profile model. The coupling between single phonon and the electronic background is drastically reduced for temperatures bellow 40 K, fully in agreement with transport-properties measurements.[3] Alloying of $FeSb_2$ with Co and Cr also reduces the coupling, i.e., leads to the B_{1g} mode narrowing. We have also observed strong A_g symmetry mode mixing.

II. EXPERIMENT

Single crystals of $FeSb_2$, $Fe_{1-x}Co_xSb_2$, and $Fe_{1-x}Cr_xSb_2$ ($0<x\leq 0.5$) were grown using the high-temperature flux method, which is described in details in Refs. 9 and 10. Sample structure and composition were determined by analyzing the powder x-ray diffraction data of $Fe(Co,Cr)Sb_2$ single crystals collected using a Rigaku Miniflex diffractometer with Cu $K\alpha$ radiation.[4] The samples stoichiometry was determined by an energy dispersive JEOL JSM-6500 SEM microprobe. Analysis of several nominal $x=0.25$ samples showed that the uncertainty in Co and Cr concentrations among samples grown from different batches was $\Delta x=0.04$. The Raman scattering measurements were performed using Jobin Yvon T64000 Raman system in micro-Raman configuration. The 514.5 nm line of an Ar^+/Kr^+ mixed gas laser was used as an excitation source. Focusing of the laser beam was realized with a long distance microscope objective (magnification 50×). We have found that laser power level of 0.02 mW on the sample is sufficient to obtain Raman signal and, except signal to noise ratio, no changes in the spectra were observed as a consequence of laser heating by further lowering laser power. The corresponding excitation power density was less then 0.1 kW/cm^2. All Raman scattering measurements presented in this work were performed using the $(10\bar{1})$ plane of $FeSb_2$ orthorhombic crystal structure. Low-temperature measurements were performed between 15 and 300 K using KONTI CryoVac continuous Helium flow cryostat with 0.5-mm-thick window.

III. RESULTS AND DISCUSSION

$FeSb_2$ crystallizes in the orthorhombic marcasite-type structure of the centrosymmetric $Pnnm$ (D_{2h}^{12}) space group, with two formula units ($Z=2$) per unit cell.[4] Basic structural unit is built up of Fe ion surrounded by deformed Sb octahedra. These structural units form edge-sharing chains along the c axis. According to the factor-group analysis there are

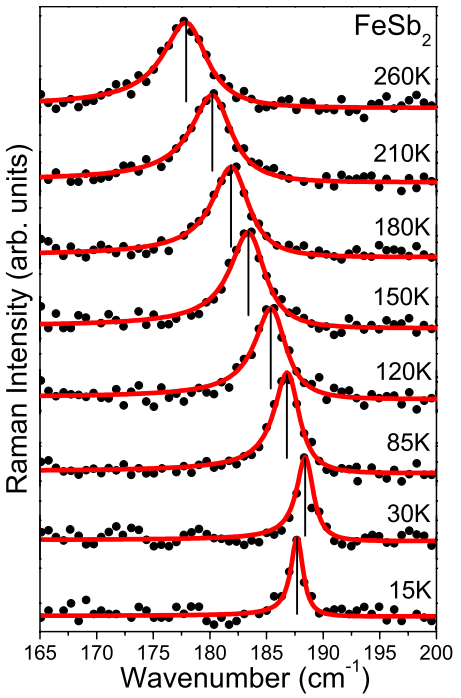

FIG. 1. (Color online) The Raman scattering spectra of $FeSb_2$ single crystals in the $(x'y)$ configuration (B_{1g} symmetry modes) measured at different temperatures.

six Raman active modes ($2A_g+2B_{1g}+B_{2g}+B_{3g}$), which were observed and assigned in our previous work.[7] The A_g and B_{1g} symmetry modes are bond stretching vibrations, whereas the B_{2g} and B_{3g} symmetry modes represent librational ones.[11]

Figure 1 shows Raman scattering spectra of $FeSb_2$ single crystals in the $(x'y)$ configuration ($x'=\frac{1}{\sqrt{2}}[101], y=[010]$) (Ref. 7) measured at different temperatures in the spectral range of the highest energy B_{1g} symmetry mode. For this configuration B_{1g} and B_{3g} modes are Raman active, see Ref. 7. One can notice an asymmetry of the B_{1g} mode toward lower wave numbers. This broad, asymmetric structure is analyzed using a BWF interference model.[12,13] The resonance usually involves an interference between Raman scattering from continuum excitations and that from a discrete phonon, provided two Raman active excitations are coupled. The BWF model line shape is given by

$$I = I_0 \frac{(1-\epsilon/q)^2}{1+\epsilon^2}, \tag{1}$$

where $\epsilon=(\omega-\omega_p)/(\Gamma/2)$ and $1/q$ is the degree of coupling which describes the departure of the line shape from a symmetric Lorentzian function. The I_0 is the intensity and ω_p and $\Gamma/2$ are the real and imaginary part of phonon self-energy, respectively. The spectra calculated using Eq. (1) are shown as solid lines in Fig. 1. The best-fit parameters are presented in Table I. Decrease in q indicates an increase in electron-phonon coupling. Nearly the same value for q above 40 K (Table I) corresponds to temperature-independent electron-phonon interaction contribution (see Fig. 2). These results are completely in agreement with the transport-properties measurements which also showed that carriers concentration

TABLE I. Parameters obtained by fitting of the B_{1g} symmetry mode spectra of pure $FeSb_2$ with the BWF line-shape model.

Temperature (K)	ω_p (cm^{-1})	Γ (cm^{-1})	q
15	187.7(2)	1.4(3)	16(1)
30	188.4(1)	1.8(3)	12(1)
85	187.0(1)	2.7(2)	9.6(8)
120	185.6(1)	3.3(3)	9.8(9)
150	183.6(1)	3.8(3)	9.8(9)
180	182.1(1)	3.9(3)	9.9(9)
210	180.4(1)	4.3(3)	9.8(9)
260	178.1(1)	4.7(3)	9.8(8)

rapidly decreases for $T<40$ K and is nearly constant above this temperature.[3]

In general, structural disorder, isotopic and/or anharmonic effects, and electron-phonon interaction can cause a change of linewidth, among which only the last two can introduce temperature dependence. Figure 2 shows temperature dependence of energy and linewidth of the B_{1g} mode for pure $FeSb_2$ sample experimentally obtained as peak position and full width at half maximum (FWHM) of the Raman mode, respectively. As can be seen from Fig. 2, in the temperature range between 15 and 40 K, the linewidth drastically increases with temperature increase. Because the phonon linewidth change due to the phonon-phonon interactions (anharmonicity) is usually very small at low temperatures we concluded that dramatic change in B_{1g} mode linewidth of $FeSb_2$ below 40 K comes from strong temperature dependent electron-phonon interaction. Support for this conclusion we found in a perfect mapping of the FWHM and $1/q$ temperature dependence for $T<40$ K and the transport-properties measurements,[3] which shows dramatic carrier concentration decrease for $T<40$ K. At higher temperatures (in our case above 40 K) major contribution to the temperature dependence of the linewidth comes from the phonon-phonon interaction because the electron-phonon contribution for $T>40$ K is temperature independent ($1/q\sim$const.).

Having this in mind, for $T>40$ K we consider energy and linewidth change in the B_{1g} mode vs temperature as pure

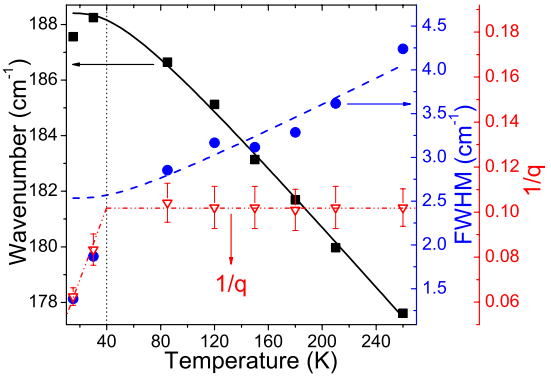

FIG. 2. (Color online) Wave number, FWHM, and the degree of coupling $(1/q)$ of the B_{1g} mode as a function of temperature for $FeSb_2$ sample.

TABLE II. Best-fitting parameters for FWHM and wave-number temperature dependence of the B_{1g} symmetry mode using Eqs. (2) and (3).

Compound	Γ_0 (cm^{-1})	A (cm^{-1})	Ω_0 (cm^{-1})	C (cm^{-1})
$FeSb_2$	2.0(2)	0.53(4)	192.4(3)	3.8(1)
$Fe_{0.75}Co_{0.25}Sb_2$	1.1(1)	0.25(2)	189.9(2)	1.80(6)
$Fe_{0.55}Co_{0.45}Sb_2$	1.5(1)	0.09(4)	190.9(2)	1.25(6)
$Fe_{0.75}Cr_{0.25}Sb_2$	0.8(2)	0.43(7)	183.2(3)	1.93(11)
$Fe_{0.5}Cr_{0.5}Sb_2$	1.4(1)	0.26(5)	176.2(3)	0.64(11)

temperature-induced anharmonic effect. Influence of the anharmonic effects on the Raman mode linewidth and energy can be taken into account via three-phonon processes[14,15]

$$\Gamma(T) = \Gamma_0 + A\left(1 + \frac{2}{e^x - 1}\right), \tag{2}$$

where Γ_0 includes intrinsic linewidth, structural disorder, isotopic effect, and temperature-independent electron-phonon interaction contribution. A is the anharmonic constant and $x = \hbar\Omega_0 / 2k_B T$.

Phonon energy is given by

$$\Omega(T) = \Omega_0 - C\left(1 + \frac{2}{e^x - 1}\right), \tag{3}$$

where Ω_0 is temperature-independent contributions, C is the anharmonic constant.[14,15] Eqs. (2) and (3) give a rather good fit (dashed and solid lines in the Fig. 2, respectively) of the experimental data for the temperature region above 40 K. Fit parameters are presented in the Table II.

From the BWF analysis of the experimental data for $Fe_{1-x}(Co,Cr)_xSb_2$ (solid lines at the right panel of Fig. 3), one can see a large increase in the q with an increase in x, indicating a decrease in electron-phonon interaction by Co and Cr alloying. Temperature dependence of energy and linewidth for $Fe_{1-x}(Co,Cr)_xSb_2$ alloys are shown in the left panel of Fig. 3. Experimental data are represented by symbols. Calculated spectra, obtained using Eqs. (2) and (3), are represented by dashed and solid lines. Best-fit parameters are presented in Table II. Γ_0 decreases significantly in $Fe_{1-x}(Co,Cr)_xSb_2$ alloys compared to the pure $FeSb_2$ (Table II), although crystal disorder increases with increasing Co and Cr concentration (for $x \leq 0.5$). This is a consequence of drastic decrease in electron-phonon interaction contribution with increasing x. One can also notice that values of anharmonic constants decrease with increasing Co and Cr concentrations, what can be a consequence of change of electronic structure of material by alloying.

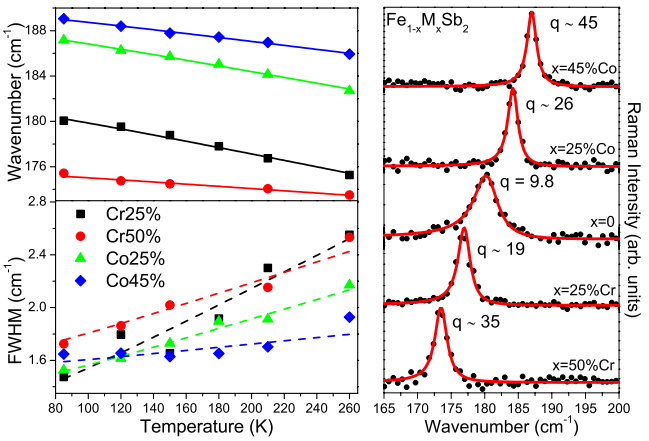

FIG. 3. (Color online) Wave number and FWHM as a function of temperature (left panel) and the BWF analysis at 210 K (right panel) of the B_{1g} mode for $Fe_{1-x}(Co,Cr)_xSb_2$ alloy samples.

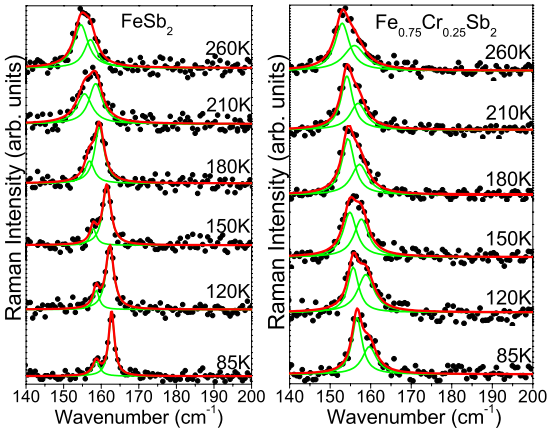

FIG. 4. (Color online) The Raman scattering spectra of $FeSb_2$ (left panel) and $Fe_{0.75}Cr_{0.25}Sb_2$ (right panel) single crystals in the $(x'x')$ configuration (A_g symmetry modes) measured at different temperatures.

The polarized Raman scattering spectra for pure $FeSb_2$ and $Fe_{0.75}Cr_{0.25}Sb_2$ single crystals in the $(x'x')$ configuration (A_g symmetry modes) measured at different temperatures, are presented in Fig. 4. We have observed structure at about 155 cm^{-1} which shows asymmetry toward higher wave numbers. However, this asymmetry cannot be ascribed to the electron-phonon interaction but is a consequence of the existence of two A_g symmetry modes, as we have already reported in our previously published paper.[7] Low-temperature measurement confirmed our previous assignation. The Lorentzian line-shape profile has been used for extraction of mode energy and linewidth. These modes have nearly the same energies what imposes the existence of the mode mixing, manifested by energy and intensity exchange. The mixing is specially pronounced when the intensities of the modes are nearly the same.[16] For $FeSb_2$ the mixing is strongest in the temperature range between 200 and 250 K and for $Fe_{0.75}Cr_{0.25}Sb_2$ between 120 and 180 K, see Fig. 4.

IV. CONCLUSION

The temperature study of polarized Raman scattering spectra of the $Fe_{1-x}M_x$ Sb_2 (M=Cr,Co) single crystals has been performed. The linewidths and energies of the Raman

modes were analyzed as a function of x and temperature. Strong electron-phonon interaction, observed for the B_{1g} symmetry mode of pure $FeSb_2$, produces significant mode asymmetry. The coupling constant reaches highest value at about 40 K and after that remains temperature independent. Additional broadening comes from the temperature-induced anharmonicity. With increasing concentration of Co and Cr in $Fe_{1-x}(Co,Cr)_xSb_2$ alloys the electron-phonon interaction is drastically reduced. We have also observed mixing of the A_g symmetry phonon modes in pure and Cr-doped sample.

ACKNOWLEDGMENTS

We have the pleasure to thank Zorana Dohčević-Mitrović for helpful discussion. This work was supported by the Serbian Ministry of Science and Technological Development under Project No. 141047. Part of this work was carried out at the Brookhaven National Laboratory which is operated for the Office of Basic Energy Sciences, U.S. Department of Energy by Brookhaven Science Associates (Grant No. DE-Ac02-98CH10886).

*Present address: Ames Laboratory and Department of Physics and Astronomy, Iowa State University, Ames, Iowa 50011, USA.

[1] C. Petrovic, J. W. Kim, S. L. Bud'ko, A. I. Goldman, P. C. Canfield, W. Choe, and G. J. Miller, Phys. Rev. B **67**, 155205 (2003).

[2] A. Bentien, S. Johnsen, G. K. H. Madsen, B. B. Iversen, and F. Steglich, EPL **80**, 39901 (2007).

[3] R. Hu, V. F. Mitrović, and C. Petrovic, Appl. Phys. Lett. **92**, 182108 (2008).

[4] R. Hu, V. F. Mitrović, and C. Petrovic, Phys. Rev. B **74**, 195130 (2006).

[5] C. Petrovic, Y. Lee, T. Vogt, N. Dj. Lazarov, S. L. Bud'ko, and P. C. Canfield, Phys. Rev. B **72**, 045103 (2005).

[6] R. Hu, V. F. Mitrović, and C. Petrovic, Phys. Rev. B **76**, 115105 (2007).

[7] N. Lazarević, Z. V. Popović, R. Hu, and C. Petrovic, Phys. Rev. B **80**, 014302 (2009).

[8] A.-M. Racu, D. Menzel, J. Schoenes, M. Marutzky, S. Johnsen, and B. B. Iversen, J. Appl. Phys. **103**, 07C912 (2008).

[9] Z. Fisk and J. P. Remeika, in *Handbook on the Physics and Chemistry of Rare Earths*, edited by K. A. Gschneider and J. Eyring (Elsevier, Amsterdam, 1989), Vol. 12.

[10] P. C. Canfield and Z. Fisk, Philos. Mag. B **65**, 1117 (1992).

[11] E. Kroumova, M. I. Aroyo, J. M. Perez Mato, A. Kirov, C. Capillas, S. Ivantchev, and H. Wondratschek, Phase Transitions **76**, 155 (2003).

[12] M. V. Klein, in *Light Scattering in Solids I*, edited by M. Cardona (Springer-Verlag, Berlin, 1983), pp. 169–172.

[13] P. C. Eklund, G. Dresselhaus, M. S. Dresselhaus, and J. E. Fischer, Phys. Rev. B **16**, 3330 (1977).

[14] M. Balkanski, R. F. Wallis, and E. Haro, Phys. Rev. B **28**, 1928 (1983).

[15] M. Cardona and T. Ruf, Solid State Commun. **117**, 201 (2001).

[16] M. N. Iliev, M. V. Abrashev, J. Laverdière, S. Jandl, M. M. Gospodinov, Y.-Q. Wang, and Y.-Y. Sun, Phys. Rev. B **73**, 064302 (2006).